Int. J. Therm. Sci. (2001) 40, 255–261

S1290-0729(00)01215-1/FLA

Performance and emissions characteristics of a partially insulated gasoline engine

Siew Hwa Chan *
School of Mechanical and Production Engineering, Nanyang Technological University, Nanyang Avenue, Singapore 639798

(Received 18 November 1999, accepted 12 April 2000)

Abstract — This paper presents the work continued from the previous study on a low heat rejection (LHR) engine. Instead of using a single-property yttria-stabilized zirconia (YSZ) coating to achieve the thermal barrier for the piston crown, a varying-properties functionally graded material (FGM) was used in this study. Extensive experiments were conducted on a 3-cylinder SI Daihatsu engine with all piston crowns coated with a layer of ceramic, which consists of zirconia and yttria with varying compositions along its thickness. Measurements of engine performance, in particular its fuel consumption and emissions characteristics, were made before and after the application of FGM coatings onto the piston crowns. To gain more insight of improved engine performance, in-cylinder pressure measurements were conducted which provide direct comparison of pressure–volume diagrams between baseline and that coated with FGM. © 2001 Éditions scientifiques et médicales Elsevier SAS

low heat rejection / thermal barrier coating / functionally-graded material / gasoline engine / performance and emissions

1. INTRODUCTION

Thermal barrier coatings (TBCs) have been successfully applied to the internal combustion engine, in particular the combustion chamber, to simulate adiabatic engines. The objectives are not only for reduced in-cylinder heat rejection and thermal fatigue protection of underlying metallic surfaces, but also for possible reduction of engine emissions [1–6]. The application of TBC reduces the heat loss to the engine cooling-jacket through the surfaces exposed to the heat transfer such as cylinder head, liner, piston crown and piston rings. The insulation of the combustion chamber with ceramic coating affects the combustion process and, hence, the performance and exhaust emissions characteristics of the engines [7–10]. The former is easily understood from the first law of thermodynamics though the reduced in-cylinder heat rejection which may not favorably convert to useful mechanical work but rather as an increased waste heat in the engine exhaust. The latter is extremely complicated as the increased air (or fuel–air mixture) temperature due to TBC (before the onset of combustion) could alter the ignition characteristic of the fuel–air mixture and its subsequent reaction mechanism which are directly related to the exhaust emissions characteristics. In addition, thermophysical properties of the coated ceramic and its surface roughness and porous characteristic, either in terms of pore size or porosity, have a direct influence on the unburned or partially burnt hydrocarbons through the effect of surface quenching and retention residual in the pores [11, 12].

On the other hand, the desire to increase the thermal efficiency or reduce fuel consumption of engines leads to the adoption of higher compression ratios, in particular for diesel engines, and reduced in-cylinder heat rejection. Both of these factors cause increased mechanical and thermal stresses of materials used in the combustion chamber. In particular for the latter, durability concerns for the materials and components in the engine cylinders, which include pistons, rings, liners and the cylinder heads, limit the maximum in-cylinder temperatures. The application of thin TBC to the surfaces of these components enhances high temperature durability by reducing the heat transfer and lowering temperature of the underlying metal [13].

In this project, the main emphasis is placed on the study of the effect of functionally-graded material coated piston crowns on the engine fuel consumption and emis-

* Correspondence and reprints.
E-mail address: mshchan@ntu.edu.sg (S.H. Chan).

sions characteristics. The optimization of engine cycles is not the concern in the present study. Emission measurements of carbon monoxide (CO), unburned hydrocarbons (uHC) and oxides of nitrogen (NO_x) are conducted in this study. Previous work [14] showed that with TBC the exhaust gas temperatures of the partially insulated engine at various operating conditions were lower than those baseline ones (without coating) which against the general belief that exhaust gas temperature should be higher for an insulated engine. In the present study, partially insulated combustion chamber with FGM coating approach is adopted which can serve the purpose of double confirming the effect of TBC coating on the exhaust gas temperature in a typical gasoline engine.

2. THERMAL BARRIER COATING (TBC) AND FUNCTIONALLY GRADED MATERIAL (FGM)

2.1. Thermal barrier coating with yttria-stabilized zirconia

The author's study has revealed that zirconia ceramics can become very strong and tough at room temperature by controlling the phases during the fabrication process. Understanding of the phase transitions is crucial to determine the required properties of zirconia ceramics. The zirconium dioxide (ZrO_2) has a monoclinic crystallographic structure at ambient temperatures. Upon raising the temperature the oxide undergoes the phase transitions from monoclinic to tetragonal with transition temperature of 1 170 °C, from tetragonal to cubic with transition temperature of 2 370 °C and from cubic to liquid with transition temperature of 2 680 °C. The transformation from tetragonal to monoclinic phase with decreasing temperature at approximately 1 170 °C is quite disruptive and renders pure ZrO_2 unusable as a high-temperature structural ceramic. This disruption is caused by a 6.5 % of volume expansion upon the transformation from tetragonal to monoclinic phase; a change which could cause structural failure of any ceramic coating.

However, ZrO_2 forms solid solutions with aliovalent oxides such as CaO, MgO, Y_2O_3 and other oxides of rare earth. This can be achieved by intimate mixing of the powders (ZrO_2 and Y_2O_3 are used in this study) and the sample is pressed to form a solid body and sintering at the temperature sufficiently high to promote the inter-diffusion of the cations. This solid solution (yttria-doped zirconia) behaves quite differently from the pure ZrO_2 as the high temperature phases, tetragonal and cubic, tend to be stabilized at temperatures lower than 1 170 °C and 2 370 °C, respectively. Hence, doping of the aforementioned aliovalent oxides serves as the stabilizing agent for the zirconia. With the addition of sufficient fraction of stabilizer, the cubic phase could be stabilized at the ambient temperature. The addition of 9 % mole fraction of yttria (Y_2O_3) or more to ZrO_2 will result in fully stabilized zirconia (FSZ) which has the cubic structure at all temperatures from ambient upwards. Addition of 6 % mole fraction of Y_2O_3 or less generates partially stabilized zirconia (PSZ) which consists of the cubic matrix with dispersed tetragonal or monoclinic precipitates, or both, depending on the temperature history in the sintering process.

2.2. Functionally graded material

Based on the considerations of phase stability in zirconia and thermal/mechanical compatibility between the coating (the thermal barrier coat) and coated (the underlying aluminium alloy) materials of the piston crown, the functionally graded material (FGM), whose properties are varied along the thickness of the coat, is considered. In this study, the FGM is actually a layer of ceramic consisting of zirconia with different proportions of yttria doping along its thickness. Functionally graded materials (FGMs) display continuously varying compositions and/or microstructures over definable geometric orientations and distances. The grades can be continuous on a microscopic level or they can be laminates comprised of gradients of metals, ceramics, polymers or variations in porosity/density. Several processing techniques have been exploited for the fabrication of FGM for structural applications: e.g., powder metallurgy, plasma spraying, *in situ* synthesis, self-propagating high temperature synthesis, reactive infiltration, etc. Physical and chemical vapour deposition techniques are also being explored to process FGM films with nanometer level composition gradients. In this study, plasma spray is used and the FGM is laminated by four sub-layers of zirconia–yttria with varying compositions from a pure zirconia ceramic to 25 %-zirconia/75 %-yttria ceramic (see *table I*).

Plasma spray processing offers a flexible and relatively economic means for producing FGM. It has been used for many years to apply layered and graded deposits (bond coats) to enhance the survivability of thick-ceramic thermal barrier coatings used in heat engines. These graded coatings are applied to reduce discontinuities in thermal expansion coefficients in order to avoid mismatch-related failure in service.

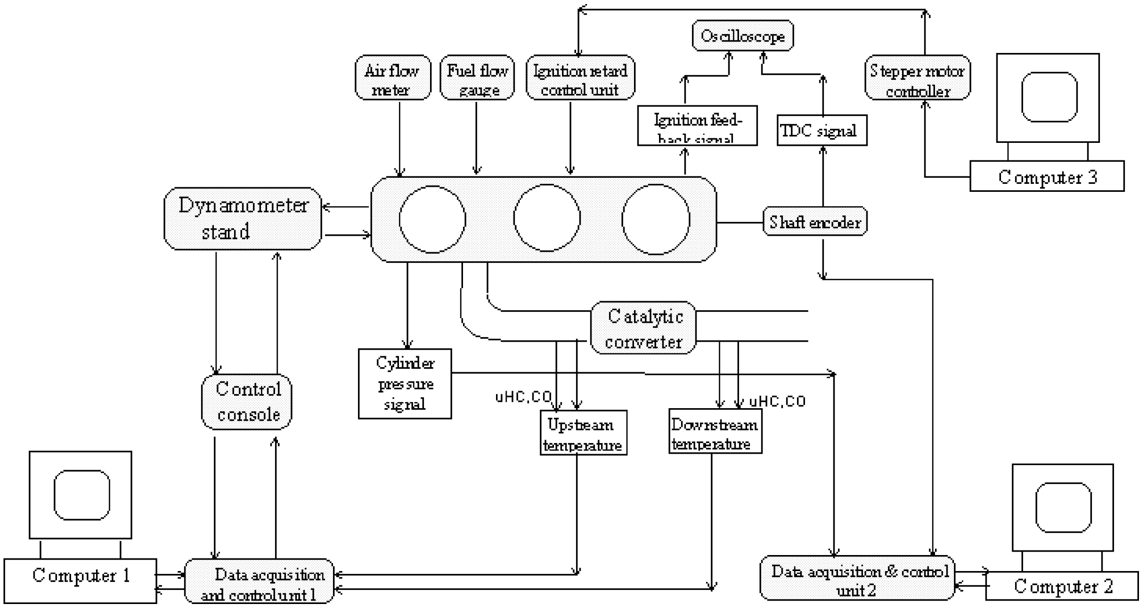

Figure 1. Schematic of engine test bed arrangement.

TABLE I
Properties of FGM coating.

Description	Density [g·m^{-3}]	Porosity [%]	Elastic modulus [GPa]
100 % ZrO_2	6.0374	12.16	53
75 % ZrO_2/25 % Y_2O_3	6.2076	11.20	105
50 % ZrO_2/50 % Y_2O_3	6.6264	10.01	158
25 % ZrO_2/75 % Y_2O_3	6.9599	8.91	187

Before applying the thermal barrier coating in a manner of "functionally graded" onto the piston crowns, a thickness of 600 µm of a new set of piston crowns was machined off. A bond coat of 150 µm and a FGM coat of 450 µm were then applied onto the piston crown by plasma spraying using a robot arm. The application of TBC is only restricted to the piston crowns in this study as the surface constitutes major part of the combustion chamber surfaces exposed to high temperature gases during combustion. The author understands that when thermal insulation is applied only to a certain part of the combustion chamber, it would undoubtedly increase the thermal loading of the others due to the increase in gas temperature. Extension of surface coating to other parts of the engine components is under exploration.

3. EXPERIMENTAL SETUP

A fully instrumented SI Daihatsu engine was mounted on a computer-controlled engine dynamometer. *Table II* tabulates the specifications of the engine while *figure 1* shows the schematic of the overall arrangement of the engine test bed.

To appreciate the effect of FGM thermal barrier coating on the engine performance, in particular the fuel consumption, obtaining engine indicator diagrams is necessary. A 10 mm water-cooled Kistler piezoeletric pressure transducer was used to measure the dynamic cylinder pressure. Unfortunately, the compact cylinder head design of the production engine does not allow

TABLE II
Specifications of the engine.

Type	gasoline, 4 cycle
Cylinder number and arrangement	3-cylinder, in-line, mounted transversely
Cylinder liner type	integral with cylinder block
Total displacement, cm^3	993
Bore × stroke, mm	76 × 73
Compression ratio	9.5
Intake and exhaust layout	crossflow
Engine dimensions (length × width × height), mm	566 × 530 × 636

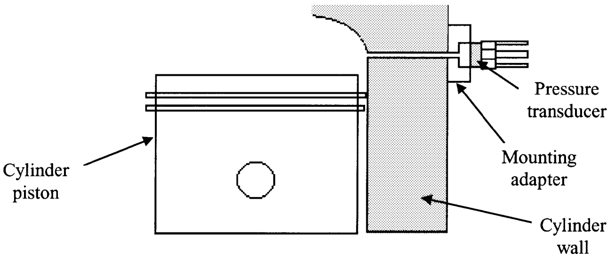

Figure 2. External mounting of pressure transducer.

the transducer of this size to be directly mounted on it, as no fill space is available for such installation. To fix the transducer, an adapter mounting is hence fabricated. A 2 mm through-hole was drilled into the third cylinder at the rear of the cylinder head to draw the pressurized gas out of the combustion chamber (see *figure 2*). This is the only place suitable for mounting the adapter, which bypasses the water jacket of the cylinder head.

In addition to the cylinder pressure measurement, a crankshaft encoder was used to trigger off the acquisition of the pressure signal and provide crank positional information. The shaft encoder possesses a resolution of 0.1° crank angle (°CA), however, the data acquisition was set to the sampling rate of 0.2 °CA.

In this experiment, a multi-gas non-dispersive infrared (NDIR) analyzer was used to measure the carbon monoxide (CO) and unburned hydrocarbons (uHC) and a chemiluminescence analyzer was used to measure the oxides of nitrogen (NO_x).

4. RESULTS AND DISCUSSIONS

Two sets of experiments were conducted and they are named as baseline tests and FGM-piston tests, respectively. In each set of tests, readings of engine speed and load, fuel consumption, exhaust gas temperature, peak cylinder pressure, concentrations of CO, uHC and NO_x, etc., were taken for engine speeds from 2 400 to 3 600 rpm with an increment of 400 rpm and engine loads from 10 to 50 Nm with an increment of 10 Nm. *Figure 3* shows the 16 test points in terms of the combination of engine speed and load. Note that the operating conditions for both baseline and FGM-piston tests were adjusted to be the same and their difference in engine power was kept within 4 %. To ensure that measurements are conducted under steady state conditions, the engine was given 10 min to stabilize when switching from one operating condition to another. All test points have been conducted twice and their average values of the measured

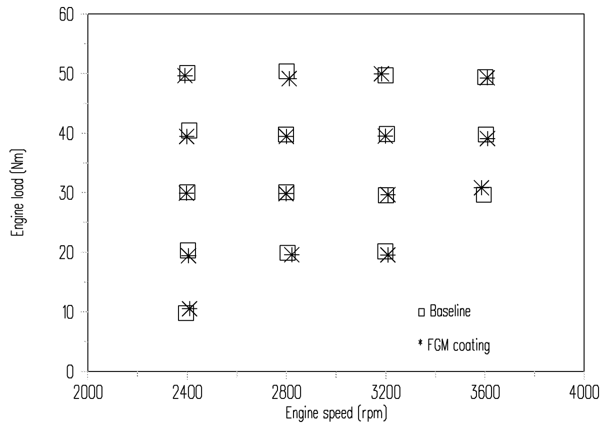

Figure 3. Layout of test points in the experiment.

parameters were used. In case the difference of measured values for a particular parameter in a test point is more than 5 %, more tests would be conducted until the difference falls within 5 % error.

In addition, for each parameter of interest, 200 readings at the sampling rate of 1 sample per second were taken (when the engine was fully warmed up) for each test point and the time average values were used for comparison. These results are collectively presented in *figures 4–10*.

Figures 4(a)–(d) show the pressure–volume diagrams, typically at 2 800 rpm, for 20, 30, 40 and 50 Nm, respectively. Analysis of the data points revealed that the ignition points of all FGM-piston tests (dotted lines) are slightly advanced relative to the baseline engine tests (solid lines). The improved ignitability of the fuel–air mixture with reduced ignition delay (pressure rise delay) causes more heat to release before the top-dead-center of the cylinder. The combined effect of the continuing compression process and the increased heat release under improved thermal insulation of the piston crowns give rise to higher cylinder pressures in the FGM-piston engine.

Figure 5 shows the comparison of peak cylinder pressures between the baseline and FGM-piston tests. The peak cylinder pressure was obtained from the sampling of cylinder pressure mentioned above, which was the ensemble average peak value of 500 cycles taken consecutively at a sampling rate of 0.2 °CA. Results show that the peak values are significantly increased in the FGM-piston tests due to the low heat rejection at the cylinder walls. The increase in trapped gases temperatures in the combustion chamber causes the increase in mean-square velocity of the gas molecules and, hence, the increase in pressure, as can be explained by the ki-

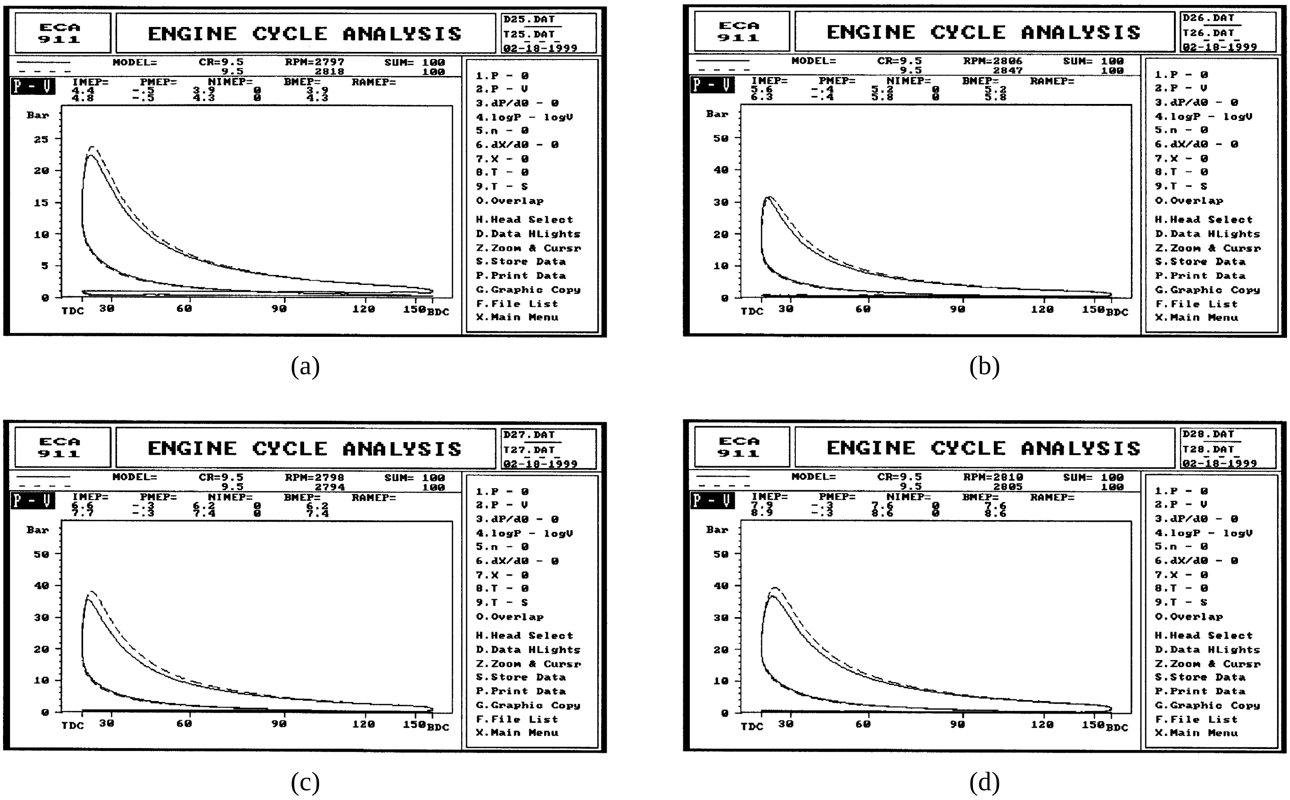

Figure 4. Pressure–volume diagrams indicating differences between baseline (solid lines) and FGM-piston (dotted lines) tests: (a) 20 Nm, (b) 30 Nm, (c) 40 Nm, (d) 50 Nm.

netic theory. Alternatively, the increase in pressure can be explained by using the ideal gas equation. However, the increase in peak cylinder pressure is not solely due to the post-ignition low heat rejection, the partially insulated combustion chamber has actually altered the ignition characteristics which has some impacts on the combustion process. The increase in peak cylinder pressure with FGM-piston is within 1 to 3 bar.

Figure 6 compares the exhaust gas temperatures between the baseline and FGM-piston tests. In general, the FGM-piston tests have shown lower exhaust gas temperatures which tally with the research work done in the previous study [14]. The increase in cylinder pressure after the top-dead-center and the reduced exhaust gas temperature in the FGM-piston engine would mean that the net work output and the thermal efficiency of the engine are both improved. Results show that the higher the engine power, the larger the difference in exhaust gas temperatures between the baseline and FGM-piston tests will be. The maximum difference registered was 38 °C at 3 600 rpm, 50 Nm.

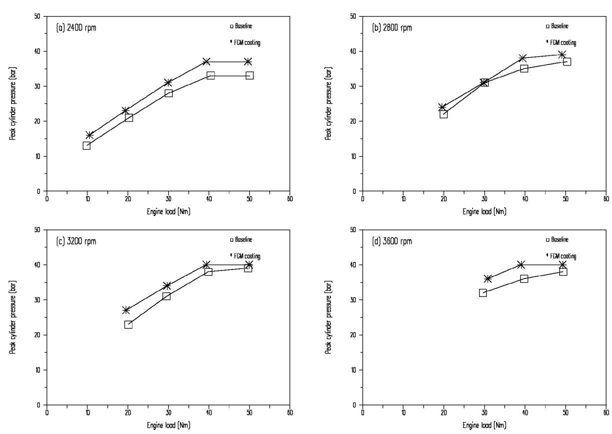

Figure 5. Effect of FGM thermal barrier coating on peak cylinder pressure. x-axis is the normalized volume but expressed as a function of degree crank angle; BDC: bottom-dead-centre; TDC: top-dead-centre.

Figure 7 compares the brake specific fuel consumption (BSFC) between the baseline and FGM-piston tests.

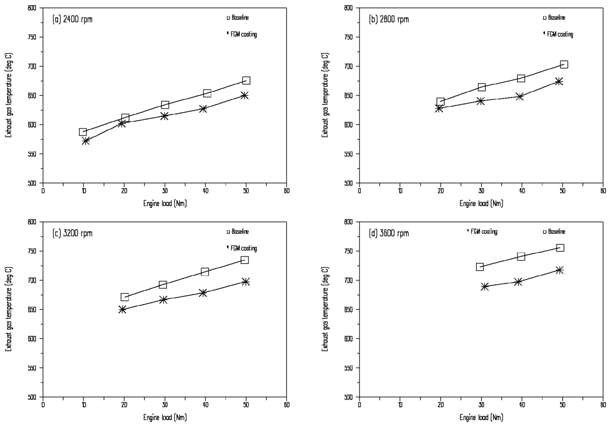

Figure 6. Effect of FGM thermal barrier coating on exhaust gas temperature.

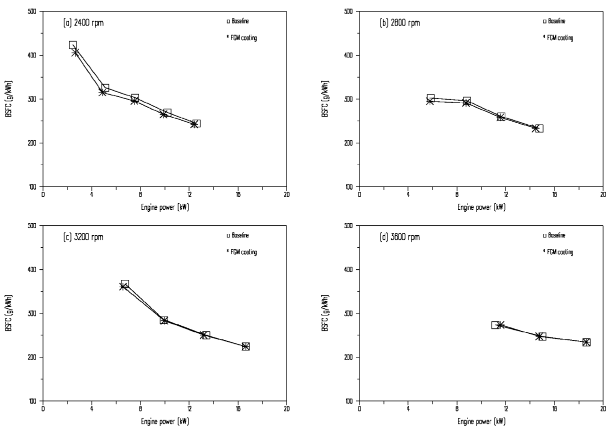

Figure 7. Effect of FGM thermal barrier coating on brake specific fuel consumption.

In general, the results show that the fuel consumption is lower in the FGM-piston engine compared under the same operating conditions. The maximum improvement of 4.8 % is at lower engine power. It is clearly seen that the improvement was diminished as engine load increased for all constant-speed tests.

Figure 8 shows the comparison of CO concentrations between the baseline and FGM-piston tests. The general trend indicates that the CO concentrations are lower with FGM-piston test. It is interesting to note that the two curves (baseline and FGM-piston tests) meet at high loads except the case of 2 800 rpm (*figure 8(b)*). The maximum difference in CO concentration is 1.25 % at 2 400 rpm, 10 Nm. Note that the resolution of the NDIR analyser used for CO measurement is 0.1 %. Except *figure 8(b)*, the trend of the curves is tally with the BSFC that less fuel consumption (relative to fixed amount of air)

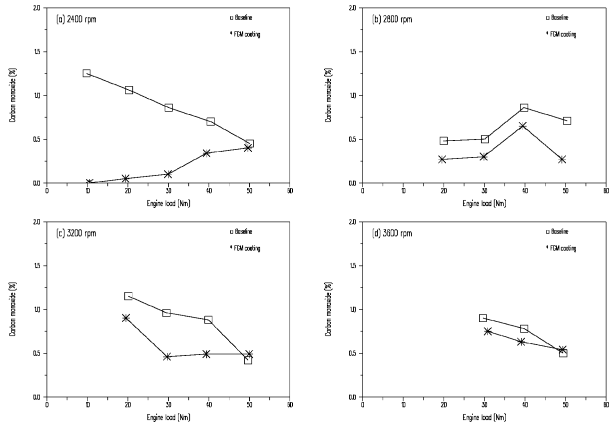

Figure 8. Effect of FGM thermal barrier coating on CO concentration.

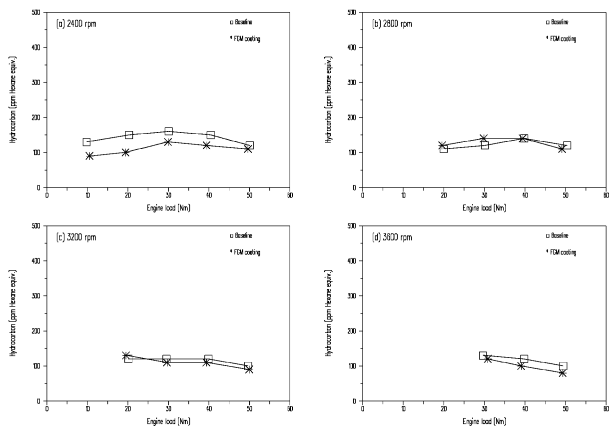

Figure 9. Effect of FGM thermal barrier coating on uHC concentration.

at low engine powers in the FGM-piston engine would contribute less CO in the exhaust. However, *figure 3* shows that at time the experiment was conducted, the load level is slightly lower in the FGM-piston engine compared with the baseline test which may contribute to lower CO concentration as depicted in *figure 8(b)*.

Figure 9 shows the comparison of uHC concentrations between the baseline and FGM-piston tests. For all cases under study, the uHC concentrations are lower in the FGM-piston engine. However, this improvement is not justifiable as the resolution of the NDIR emission analyzer is 20 ppm and most of the differences in uHC between the baseline and FGM-piston tests are fall within the error band.

Figure 10 compares the NO_x concentrations between the baseline and FGM-piston tests. Results show that NO_x is significantly higher in the FGM-piston tests

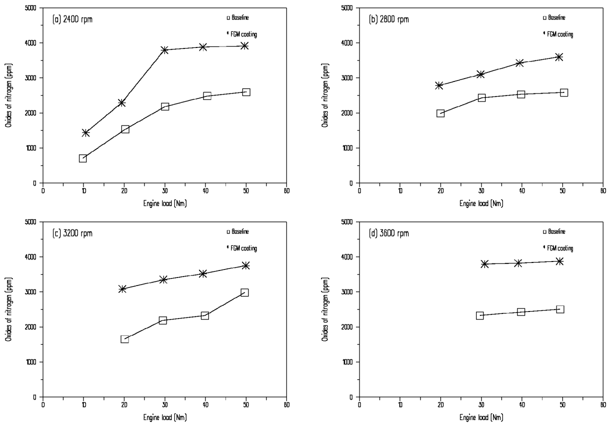

Figure 10. Effect of FGM thermal barrier coating on NO_x concentration.

which is tally with the higher cylinder pressure shown in the *p–V* diagrams (*figure 4*). The maximum difference in NO_x concentration registered was around 1 450 ppm at 3 600 rpm.

5. CONCLUSIONS

The study of the effect of FGM thermal barrier coating applied to the piston crown on the engine characteristics leads to the following conclusions:

(1) Zirconia–yttria-based functionally-graded material (FGM) has been applied successfully to the piston crowns as the thermal barrier of a small gasoline engine to prevent excessive heat loss during the combustion process.

(2) Sampling of pressures in the cylinders showed that the ignition point of the FGM-piston engine has been advanced slightly relative to the baseline engine indicating the improvement in ignitability and heat release before the top dead centre. This together with its subsequent effect on the combustion process and the reduced heat loss contributes to increased cylinder pressure and improved thermal efficiency and brake specific fuel consumption.

(3) Exhaust gas temperatures are lower with the FGM-piston tests. A maximum difference of 38 K (with baseline test) was registered at the highest engine power in the tests. The lower exhaust gas temperature was attributed to the improved energy conversion into useful mechanical work in a partially insulated engine as evident by the reduction of BSFC.

(4) Measurements of CO, uHC and NO_x concentrations indicated that CO and uHC are lower but NO_x is higher in the FGM-piston tests. However, the improvement in the uHC is not so justifiable as the differences in concentration are around 20 ppm, which are fall within the resolution of the NDIR analyzer used. The increase in NO_x level by around 1 400 ppm with the FGM-piston tests is significant which is the common problem associated with insulated engines.

REFERENCES

[1] French C.C.J., Ceramics in reciprocating internal combustion engines, SAE Paper No. 841135, 1984.

[2] Moore Ch.H., Hoehne J.L., Combustion chamber insulation effect on the performance of a low heat rejection Cummins V-903 engine, SAE Paper No. 860317, 1986.

[3] Churchill R.A., Smith J.E., Clark N.N., Turton R.A., Low-heat rejection engines — A concept review, SAE Paper No. 880014, 1988.

[4] Harris D.H., Lutz J., Thermal barrier coatings — Technology for diesel engines, SAE Paper No. 880437, 1988.

[5] Reddy C.S., Domingo N., Graves R.L., Low heat rejection engine research status: Where do we go from here?, SAE Paper No. 900620, 1990.

[6] Yonushonis T.M., Overview of thermal barrier coatings in diesel engines, J. Thermal Spray Technology 6 (1) (1997) 50–56.

[7] Sudhakar V., Performance Analysis of Adiabatic Engine, SAE Paper No. 840431, 1984.

[8] Assanis D., Wiese K., Schwarz E., Bryzik W., The effects of ceramic coatings on diesel engine performance and exhaust emissions, SAE Paper No. 910460.

[9] Kimura S., Matsui Y., Itoh T., Effects of combustion chamber insulation on the heat rejection and thermal efficiency of diesel engines, SAE Paper No. 920543, 1992.

[10] Schwarz E., Reid M., Bryzik W., Danielson E., Combustion and performance characteristics of a low heat rejection engine, SAE Paper No. 930988, 1993.

[11] Frank R.M., Heywood J.B., The effect of piston temperature on hydrocarbon emissions from a spark-ignited direct-injection engine, SAE Paper No. 910558, 1991.

[12] Wentworth J.T., More on origins of exhaust hydrocarbons — Effects of zero oil consumption, deposit location and surface roughness, SAE Paper No. 920939, 1992.

[13] Haselkorn M.H., Wear-resistant ceramic coatings for diesel engines, J. Thermal Spray Technology 4 (1995).

[14] Chan S.H., Khor K.A., The effect of thermal barrier coated piston crown on engine characteristics, J. Mat. Eng. Perf. 9 (1) (2000) 103–109.